

# Determination of the neutrino mass ordering by combining PINGU and Daya Bay II

Mattias Blennow<sup>\*</sup>, Thomas Schwetz<sup>†</sup>,

<sup>\*</sup> *Department of Theoretical Physics, School of Engineering Sciences, KTH Royal Institute of Technology, AlbaNova University Center, 106 91 Stockholm, Sweden*

<sup>†</sup> *Max-Planck-Institut für Kernphysik, Saupfercheckweg 1, 69117 Heidelberg, Germany*

## Abstract

The relatively large measured value of  $\theta_{13}$  has opened various possibilities to determine the neutrino mass ordering, among them using PINGU, the low-energy extension of the IceCube neutrino telescope, to observe matter effects in atmospheric neutrinos, or a high statistics measurement of the neutrino energy spectrum at a reactor neutrino experiment with a baseline of around 60 km, such as the Daya Bay II project. In this work we point out a synergy between these two approaches based on the fact that when data are analysed with the wrong neutrino mass ordering the best fit occurs at different values of  $|\Delta m_{31}^2|$  for PINGU and Daya Bay II. Hence, the wrong mass ordering can be excluded by a mismatch of the values inferred for  $|\Delta m_{31}^2|$ , thanks to the excellent accuracy for  $|\Delta m_{31}^2|$  of both experiments. We perform numerical studies of PINGU and Daya Bay II sensitivities and show that the synergy effect may lead to a high significance determination of the mass ordering even in situations where the individual experiments obtain only poor sensitivity.

---

<sup>\*</sup>emb AT kth.se

<sup>†</sup>schwetz AT mpi-hd.mpg.de

# 1 Introduction

Experiments with atmospheric neutrinos and reactor antineutrinos have played a crucial role for our current understanding of neutrino oscillations. The first evidence for neutrino oscillations was obtained by the observation of the zenith angle dependent disappearance of atmospheric muon neutrinos in SuperKamiokande [1]. The KamLAND reactor experiment provided an independent confirmation of solar neutrino oscillations [2] and obtained strong evidence for the spectral distortion as predicted by oscillations [3]. Various reactor experiments also played a crucial role in the determination of the last unknown mixing angle  $\theta_{13}$  [4–7]. Combining those with other data on oscillations [8–10] we now have a good picture of the neutrino mass pattern and the leptonic mixing matrix, see [11] for a global fit. One of the big remaining questions is the type of the neutrino mass ordering, which can be “normal” or “inverted”, depending on the sign of the neutrino mass-squared difference  $\Delta m_{31}^2$  responsible for the above mentioned muon neutrino disappearance. Indeed, there is a chance that atmospheric and/or reactor neutrinos again may play a crucial role in answering this question.

In atmospheric neutrino experiments, the determination of the mass ordering is based on the matter effect [12–14] in  $\Delta m_{31}^2$  driven oscillations, see [15] for a recent review. In case of normal ordering ( $\Delta m_{31}^2 > 0$ ) the MSW resonance will occur for neutrinos, whereas for the inverted ordering ( $\Delta m_{31}^2 < 0$ ) it will happen for antineutrinos. Atmospheric neutrinos with baseline lengths up to the full diameter of the earth provide an interesting opportunity to study this effect. One possibility is to invoke a magnetic field to separate neutrino- and antineutrino-induced muons. This approach is pursued by the ICal@INO experiment [16], for recent sensitivity studies see [17, 18]. In the absence of a magnetic field no discrimination between neutrino- and antineutrino-induced events is possible on an event-by-event basis, and therefore the effect of changing the neutrino mass ordering is strongly diluted. However, a non-zero net effect remains, since neutrinos and antineutrinos do not contribute equally to the total event sample due to different interaction cross sections. In huge detectors with several Mt yr exposures those subtle effects are observable and provide sensitivity to the neutrino mass ordering. This possibility is discussed in the context of neutrino telescopes such as IceCube and ANTARES/KM3NET under the acronyms PINGU (Precision IceCube Next-Generation Upgrade) [19] and ORCA (Oscillation Research with Cosmics in the Abyss) [20], respectively, or for huge underground detectors [21, 22].

A very different method to determine the neutrino mass ordering has been pointed out in [23]. In a reactor experiment close to the first oscillation maximum of  $\Delta m_{21}^2$  (at a baseline around 60 km), oscillations driven by  $\Delta m_{31}^2$  and  $\theta_{13}$  manifest themselves as small wiggles in the energy spectrum. The effect of the neutrino mass ordering enters via a subtle interference effect in the  $\bar{\nu}_e \rightarrow \bar{\nu}_e$  survival probability between oscillations due to  $\Delta m_{31}^2$  and  $\Delta m_{21}^2$ . The basic observation is that the amplitudes of oscillations with  $\Delta m_{31}^2$  and  $\Delta m_{32}^2$  are different, due to the large but non-maximal value of  $\theta_{12}$ . Furthermore,

for normal ordering  $|\Delta m_{31}^2| > |\Delta m_{32}^2|$ , whereas for inverted ordering  $|\Delta m_{31}^2| < |\Delta m_{32}^2|$ . Hence, by finding out whether the larger or the smaller frequency in the energy spectrum has the larger or smaller amplitude one can determine the mass ordering. The possibilities for exploring this effect are currently investigated in the context of the Daya Bay II [24,25] and the RENO50 [26] projects.

Both of these methods to determine the neutrino mass ordering are experimentally challenging. They require huge statistics as well as excellent control over energy reconstruction and for atmospheric neutrinos also directional reconstruction. Currently it is not fully established whether the necessary requirements can be met and it might happen that those experiments achieve only modest sensitivity to the mass ordering. In the following we point out an interesting way to identify the mass ordering with high significance by combining data from an atmospheric and a reactor neutrino experiment, even if the individual sensitivities are low. To be specific we will consider the PINGU and Daya Bay II setups.

The main observation is the following: when a fit to the data is performed with the wrong mass ordering, the best fit point will be located at a value  $|\Delta m_{31}^2|_{\text{wrong}}$ , which is different to the one in the correct mass ordering. Moreover, the value of  $|\Delta m_{31}^2|_{\text{wrong}}$  is different in the atmospheric and reactor neutrino experiments. It turns out that the difference between  $|\Delta m_{31}^2|_{\text{wrong}}^{\text{PINGU}}$  and  $|\Delta m_{31}^2|_{\text{wrong}}^{\text{Daya Bay II}}$  typically is larger than the uncertainties with which it will be determined by those experiments. Hence, by the mismatch of the values for  $|\Delta m_{31}^2|$  determined by the two experiments one may be able to exclude the wrong mass ordering, even if the individual  $\chi^2$  differences between the fit with the correct and the wrong ordering are small.

A similar effect has been discussed in [27, 28], where the comparison of  $\nu_\mu$  and  $\nu_e$  disappearance experiments is used to determine the mass ordering, see also [29]. The main idea is similar to our proposal of combining PINGU and Daya Bay II, however there are important differences. In [27] the focus is on disappearance experiments measuring  $\Delta m_{31}^2$  at the first oscillation maximum. The formulas derived in that reference for the effective mass-squared differences  $\Delta m_{ee}^2$  and  $\Delta m_{\mu\mu}^2$  are based on this configuration. In the experiments we are considering here the oscillation physics are somewhat more involved. For Daya Bay II the wrong  $|\Delta m_{31}^2|$  is determined by fitting the tiny wiggles on the energy spectrum with the wrong mass ordering. Some analytic considerations on the value of  $|\Delta m_{31}^2|_{\text{wrong}}^{\text{Daya Bay II}}$  can be found in [30]. Also, the oscillation physics in PINGU are more complicated than for a long-baseline  $\nu_\mu$  disappearance experiment. In PINGU a superposition of the  $\nu_e \rightarrow \nu_\mu$  and  $\bar{\nu}_e \rightarrow \bar{\nu}_\mu$  channels is observed, while also summing over neutrinos and antineutrinos. Furthermore, a wide range of energies and baselines is sampled, including resonant matter effects. This makes it more difficult to understand the location of  $|\Delta m_{31}^2|_{\text{wrong}}^{\text{PINGU}}$  analytically. We will determine the locations of the  $\chi^2$  minimum with the wrong mass ordering numerically, and indeed we do find deviations from the formulas derived in [27] comparable to the precision of  $|\Delta m_{31}^2|$ . In fact, we will see that the best fit with the wrong ordering differs from that in the correct one also when

$$\Delta m_{21}^2 = 0.$$

The combination of Daya Bay II data with an independent determination of  $|\Delta m_{31}^2|$  from MINOS or T2K has been considered in, e.g., [30–32], where a modest improvement of the sensitivity (depending on the assumed accuracy) is obtained. A combination of PINGU data with a measurement of  $|\Delta m_{31}^2|$  from T2K has been performed in Ref. [33], finding only a marginal improved mass ordering sensitivity by this combination. Indeed, both PINGU as well as Daya Bay II will both obtain unprecedented precision in the determination of  $|\Delta m_{31}^2|$  and therefore they offer the most promising combination to explore this effect for the determination of the mass ordering.

The outline of the paper is as follows. We start discussing the sensitivity of PINGU and Daya Bay II individually in sections 2 and 3, respectively, where also the details of our numerical analyses are given. In section 4 we show how an excellent sensitivity to the mass ordering can be obtained by the combination of PINGU and Daya Bay II, even when the individual experiments do not achieve a high sensitivity. We conclude in section 5.

## 2 PINGU

PINGU [19] is a low-energy extension of the IceCube neutrino telescope at the south pole, obtained by installing additional strings with digital optical modules (DOMs) within the existing DeepCore detector [34]. This would allow the observation of atmospheric neutrinos with a fiducial volume of several Mt and a threshold of a few GeV.<sup>1</sup> It has been pointed out in [38] that, with the large value of  $\theta_{13}$  that has recently been established, such a configuration has the potential to determine the neutrino mass ordering, see also [39, 40]. As discussed in detail in [38], the difference between the mass orderings is visible as a characteristic pattern in the plane of neutrino energy and direction. A crucial detector requirement is therefore a good ability to reconstruct neutrino energy and direction, see also [41–43] in the context of a magnetized detector. Recently the sensitivity of a PINGU-like configuration has been studied by a number of authors [33, 38, 44–46]. Given the importance of the issue we will also provide a further independent study of the PINGU setup, considering various options for the achieved resolutions and show the impact on the sensitivity. For the sake of definiteness we will concentrate on the capabilities of PINGU; qualitative features are expected to be similar for ORCA.

### 2.1 Event rate calculation

In this work we consider only muon-like events and assume an effective detector mass for PINGU as obtained by recent simulations of the IceCube collaboration: we adopt the effective volume times density of ice as function of neutrino energy as shown on slide 3

---

<sup>1</sup>The possibility to use such a detector as target for an artificial neutrino beam has been considered in [35–37].

of [47] by the curve labeled “Triggered Effective Volume,  $R = 100$  m”. This curve can be approximated by the expression

$$\rho_{\text{ice}} V_{\text{eff}}(E_\nu) \approx 2.4 \log \left( \frac{E_\nu}{1 \text{ GeV}} - 2 \right)^{0.87} \text{ Mt}. \quad (1)$$

The threshold is around 3 GeV and the effective mass rises to about 4 Mt at 10 GeV and 7 Mt at 35 GeV. We consider the initial neutrino flavours  $\nu_\mu, \bar{\nu}_\mu, \nu_e, \bar{\nu}_e$  and fold the fluxes with the oscillation probabilities  $P_{\nu_\mu \rightarrow \nu_\mu}, P_{\bar{\nu}_\mu \rightarrow \bar{\nu}_\mu}, P_{\nu_e \rightarrow \nu_\mu}, P_{\bar{\nu}_e \rightarrow \bar{\nu}_\mu}$ , respectively. The probabilities are obtained by numerically solving the evolution equations through a realistic Earth density profile [48].

The ability to reconstruct neutrino energy and direction is crucial to resolve the signatures induced by changing the neutrino mass ordering. The actual performance of the PINGU detector is under active investigation. Here we adopt various assumptions to show the goals which have to be achieved in order to obtain a relevant sensitivity. We consider two different approaches: muon reconstruction or neutrino reconstruction, which we describe in the following.

**Muon reconstruction.** Here we (conservatively) assume that only the muon can be reconstructed and no information from the hadron shower is used (this approach has been adopted in [45]). We implement this by an integration of the event rates based on a Monte Carlo sample of neutrino events<sup>2</sup>. Neutrino nadir angles are sampled in  $\cos \theta_\nu$  between 0 and 1 in steps of  $\Delta \cos \theta_\nu = 0.02$ . For given  $\cos \theta_\nu$  a random neutrino energy is drawn according to the atmospheric neutrino flux [49], weighted by the effective detector mass as a function of neutrino energy and the oscillation probability.

A muon is then generated with the GENIE event generator [50] assuming a water target, returning the muon energy  $E_\mu$  and the angle  $\alpha$  between the muon and the neutrino. The muon energy is smeared assuming a Gaussian detector resolution  $\sigma_{E_\mu}$  and distributed accordingly over the bins in  $E_\mu$ . We use 20 bins in  $E_\mu$  logarithmically spaced between 1 GeV and 40 GeV (note that the actual threshold is set by the effective volume function in Eq. 1). We use logarithmic bins in order to have finer binning in the low energy region, where the main information on the mass ordering is obtained. We also assume a Gaussian detector resolution  $\sigma_{\theta_\mu}$  on the muon direction. This is implemented by drawing a random angle  $\delta\alpha$  from a Gaussian distribution with width  $\sigma_{\theta_\mu}$  which we then add to the angle  $\alpha$ . We then distribute the event in bins in the muon nadir angle using the given neutrino nadir angle and the angle  $\alpha + \delta\alpha$  between neutrino and muon, assuming a flat distribution of the muon azimuthal angle with respect to the neutrino direction. We use 20 bins in  $\cos \theta_\mu$  between 0.1 and 1.

Monte Carlo events are generated for an exposure of 100 years and scaled down to the desired exposure time in order to predict the expected event numbers per bin. Even for perfect reconstruction of the muon energy and direction, a sizable smearing of the oscillation probability happens due to the kinematical relations between neutrino and

---

<sup>2</sup>We thank Anselmo Mereaglia for providing us his Monte Carlo event sample to perform this study.

muon energies/directions. We show some representative values of the muon reconstruction abilities to illustrate the impact on the sensitivity. Apart from the perfect muon detection with  $\sigma_{E_\mu} = 0$  and  $\sigma_{\theta_\mu} = 0$ , we consider also the situation of  $\sigma_{E_\mu} = 15\%$  and  $\sigma_{\theta_\mu} = 10^\circ$ .

**Neutrino reconstruction.** Most likely the assumption that no information from the hadron shower can be obtained is too pessimistic. It may be possible to reconstruct the neutrino energy and direction directly by using information from the muon track as well as the hadron shower<sup>3</sup>. Estimates on the reconstruction accuracies for neutrino properties are given in [38]. We adopt the same representative values as used there. The neutrino energy and angle reconstruction resolutions are assumed to be Gaussian with the widths

$$\sigma_{E_\nu} = A + BE_\nu, \quad \sigma_{\theta_\nu} = C \sqrt{\frac{1 \text{ GeV}}{E_\nu}}, \quad (2)$$

respectively. For the energy resolution we consider the two examples ( $A = 2 \text{ GeV}, B = 0$ ) and ( $A = 0, B = 0.2$ ) and for the angular resolution we take the two representative values  $C = 0.5$  and  $C = 1 \text{ rad}$ . For  $C = 0.5$  this corresponding to about  $13^\circ$  ( $9^\circ$ ) at  $E_\nu = 5 \text{ GeV}$  ( $10 \text{ GeV}$ ). For the calculation of the event rates we follow closely [42], where more details can be found. The neutrino fluxes [52] are folded with the cross section [53], the neutrino energy dependent effective detector mass, the oscillation probabilities as well as with the reconstruction resolutions described above. The same binning as for the muon data is used, except that now it is understood in terms of reconstructed neutrino quantities.

## 2.2 Statistical analysis and systematic uncertainties

We investigate the potential to determine the mass ordering by performing a statistical analysis based on a  $\chi^2$ -function. We consider the two-dimensional event distribution in either muon or neutrino nadir angle and energy. Let us denote the number of events in bin  $jk$  by  $R_{jk}(\mathbf{x})$ , where  $\mathbf{x}$  is a vector of the oscillation parameters. We calculate “data” by adopting “true values”  $\mathbf{x}^{\text{true}}$  for the oscillation parameters:  $D_{jk} = R_{jk}(\mathbf{x}^{\text{true}})$ . In the theoretical prediction we take several sources of systematic errors into account by introducing 11 pull variables  $\boldsymbol{\xi} = (\xi_1, \dots, \xi_{11})$ :

$$T_{jk}(\mathbf{x}, \boldsymbol{\xi}) = R_{jk}(\mathbf{x}) \left( 1 + \sum_{l=1}^{11} \xi_l \pi_{jk}^l \right), \quad (3)$$

with appropriately defined “couplings”  $\pi_{jk}^l$ . In the systematic error treatment we follow closely the description given in the appendix of [54], where also a definition of the  $\pi_{jk}^l$  can be found. The systematic effects included in our analysis are listed in Tab. 1. We consider a fully correlated overall normalization error of 20% from various sources

---

<sup>3</sup>In [46] also the reconstruction of the  $y$ -distribution is considered, which may in principle be used to discriminate neutrino from antineutrino events on a statistical basis. We do not follow this strategy here. According to [46] using the  $y$ -distribution leads to an increase of significance between about 10% (no degeneracy, worse resolutions) up to 42% (worse case degeneracy, best resolution). See also [51].

index $l$	systematic effect	value
1	overall normalization	20%
2	$\nu/\bar{\nu}$ ratio	5%
3	$\nu_\mu/\nu_e$ ratio of fluxes	5%
4 – 7	$\cos\theta_\nu$ dependence of fluxes	5%
8 – 11	energy dependence of fluxes	5%

Table 1: Systematic uncertainties included in our PINGU analysis.

such as uncertainties in the atmospheric neutrino fluxes, the cross sections, the fiducial detector mass, or efficiencies. Furthermore, we take into account an uncertainty in the neutrino/antineutrino ratio (including fluxes as well as cross sections) and an error on the ratio of  $e$ -like to  $\mu$ -like fluxes. In addition to these normalization errors we also allow for uncertainties in the shape of the neutrino fluxes by introducing a linear tilt in the nadir angle as well as in energy, uncorrelated between the four fluxes of  $\nu_e, \bar{\nu}_e, \nu_\mu, \bar{\nu}_\mu$ .

We adopt a  $\chi^2$ -definition based on Poisson statistics:

$$\Delta\chi^2(\mathbf{x}) = \min_{\boldsymbol{\xi}} \left[ 2 \sum_{j=1}^{N_E^{\text{bin}}} \sum_{k=1}^{N_\theta^{\text{bin}}} \left( T_{jk}(\mathbf{x}, \boldsymbol{\xi}) - D_{jk} + D_{jk} \ln \frac{D_{jk}}{T_{jk}(\mathbf{x}, \boldsymbol{\xi})} \right) + \sum_{l=1}^{11} \xi_l^2 \right]. \quad (4)$$

The dependence on  $\mathbf{x}^{\text{true}}$  is implicit via  $D_{jk}$ . In the cases of interest (PINGU and Daya Bay II) event numbers in most of the bins are large and in this case the first term of the right-hand side of eq. 4 becomes equivalent to the standard Gaussian  $\chi^2$  definition. The term including the pull parameters  $\xi_l$  assumes that systematic uncertainties behave like Gaussian errors. The sensitivity based on pure statistics (without including the effect of systematic uncertainties) is obtained by fixing the  $\xi_l$  to zero. We call eq. 4 “ $\Delta\chi^2$ ” because for  $\mathbf{x} = \mathbf{x}^{\text{true}}$  eq. 4 is zero, by definition. In order to quantify the sensitivity to the mass ordering we consider  $\Delta\chi^2(\mathbf{x})$  where the sign of  $\Delta m_{31}^2$  in  $\mathbf{x}$  is taken opposite to the one in  $\mathbf{x}^{\text{true}}$ . Whenever we quote  $\Delta\chi^2$  values for the mass ordering sensitivity we always minimize  $\Delta\chi^2(\mathbf{x})$  with respect to  $|\Delta m_{31}^2|$ , without including any external information on this parameter. We will show the impact of either fixing  $\theta_{13}$  and  $\theta_{23}$  or minimizing with respect to them. When minimizing over them we include external information on the mixing angles via adding a term  $\chi_{\text{prior}}^2$  to eq. 4, assuming a 5% error on  $\sin^2(2\theta_{13})$  as well as a 15% error on  $\sin^2(2\theta_{23})$ . If not stated otherwise we use the following true values:

$$\begin{aligned} |\Delta m_{31}^2| &= 2.4 \cdot 10^{-3} \text{ eV}^2, & \Delta m_{21}^2 &= 7.59 \cdot 10^{-5} \text{ eV}^2, \\ \sin^2 2\theta_{13} &= 0.09, & \sin^2 2\theta_{23} &= 1, & \sin^2 \theta_{12} &= 0.302, & \delta &= 0. \end{aligned} \quad (5)$$

The precise statistical meaning of sensitivity statements based on eq. 4 is non-trivial. A detailed discussion of those issues is given in [55], see also [56, 57]. One can define a test statistic which under certain conditions follows a Gaussian distribution with mean given by  $\Delta\chi^2$  from eq. 4 and standard deviation  $2\sqrt{\Delta\chi^2}$  [45, 55, 56]. In this paper we will

follow the traditional habit of saying that “the sensitivity to the mass ordering is  $n\sigma$ ” with  $n = \sqrt{\Delta\chi^2}$ . It can be shown [55] that under the above mentioned Gaussian assumption the interpretation of the statement is the following: if  $n = \sqrt{\Delta\chi^2}$  then the experiment will exclude the wrong mass ordering at  $n\sigma$  with a probability of roughly 50%. We have checked [55] that for PINGU and even more for Daya Bay II typically those assumptions are approximately fulfilled, in reasonable agreement with the results from [45] for PINGU and [30] for Daya Bay II.

### 2.3 PINGU sensitivity to the mass ordering

Let us first consider the effect of energy and directional resolutions, systematic uncertainties, and parameter degeneracies on the sensitivity to the mass ordering. For this study we will adopt the approximation  $\Delta m_{21}^2 = 0$ , motivated by the fact that we consider only neutrino energies above several GeV. In that range effects of  $\Delta m_{21}^2$  are expected to be small. In this limit the mixing angle  $\theta_{12}$  as well as the CP phase  $\delta$  become unphysical, and oscillation probabilities depend only on the three parameters  $\theta_{13}$ ,  $\theta_{23}$  and  $\Delta m^2$ , where  $\Delta m^2 \equiv \Delta m_{31}^2 = \Delta m_{32}^2$  for  $\Delta m_{21}^2 = 0$ . This approximation is necessary for practical purposes, in order to make the numerical analysis including systematic uncertainties as well as the marginalization over  $\theta_{13}$  and  $\theta_{23}$  feasible. We will discuss the effect of the CP phase  $\delta$  without adopting any approximation on the three-flavour oscillations later in this work.

In Fig. 1, we show the expected  $\Delta\chi^2$  as a function of  $|\Delta m^2|$  of the wrong mass ordering after 3 years of data and how it depends on our assumptions regarding systematic errors, marginalization of parameters, and experimental resolutions. The set of curves at smaller (larger) values of  $|\Delta m_{31}^2|$  correspond to a true normal (inverted) ordering. We note that in all cases, systematic errors will have a significant impact on the final sensitivity of the experiment. We find that the uncertainty in the oscillation parameters  $\theta_{23}$  and  $\theta_{13}$  are important only for true inverted ordering. However, once both effects have been taken into account, the effects of the other are diminished. In particular, the effect of allowing parameters to vary freely is significantly reduced once the systematic errors have been introduced. Despite the differences introduced by taking these effects into account, the most crucial assumption is the assumption on the energy and angular resolutions, with the results varying with several  $\sigma$  depending on the assumptions made (compare thin versus thick curves). It should also be clear from the figure that whether we make assumptions on the measurements of the muon parameters (left panel) or those of the reconstructed neutrino parameters (right panel), the results are relatively similar and seem to exhibit similar characteristic when it comes to the importance of systematic errors and incomplete knowledge of the neutrino parameters.

In Fig. 2, we show the sensitivity of PINGU to the mass ordering under the assumption that the normal ordering is the true one as a function of the PINGU running time. We confirm previous results that the energy and angular resolutions play a major role in the mass ordering determination (e.g., [33,38]), as does the inclusion of systematic errors.

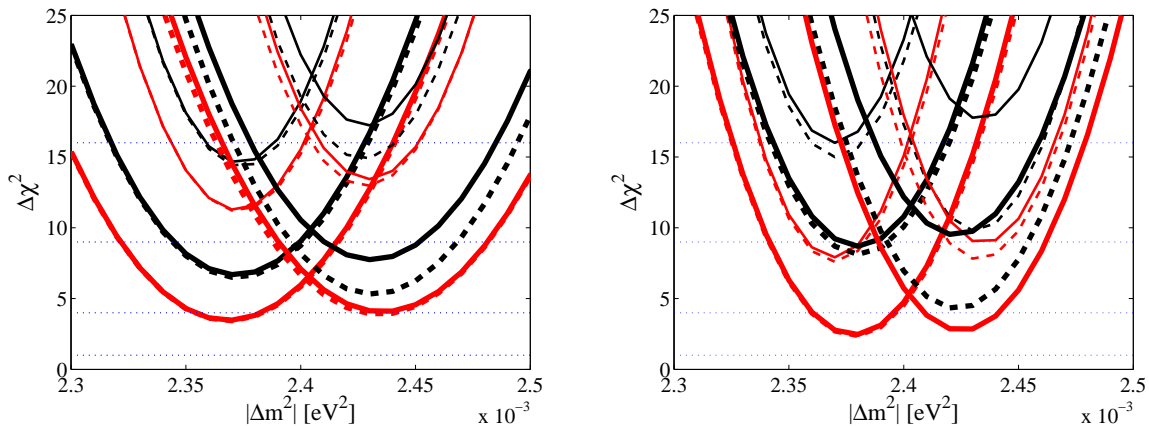


Figure 1: The expected PINGU 3-year  $\Delta\chi^2$  in the wrong ordering as a function of  $|\Delta m^2|$  (in the approximation  $\Delta m_{21}^2 = 0$ ) for the simulations involving the muon parameters (left) and for the simulations using the reconstructed neutrino parameters (right). The solid (dashed) curves correspond to simulations where the oscillation parameters were fixed to their input values (allowed to vary with a prior penalizing too large deviations from them), the black (red) curves correspond to simulations without (with) systematic errors included, and the different thickness of the curves signify different assumptions on the energy and angular resolutions. For the left panel, the resolutions were assumed to be  $\sigma_{E_\mu}/E_\mu = 0.15$  and  $\sigma_{\theta_\mu} = 10^\circ$  for the thick curves, while perfect energy and angular resolution on the muon was assumed for the thin curves. For the right panel, the resolution on the reconstructed neutrino parameters were assumed to be  $\sigma_{E_\nu} = 2 \text{ GeV}$  ( $0.2E_\nu$ ) and  $\sigma_{\theta_\nu} = \sqrt{(1 \text{ GeV})/E_\nu}$  ( $0.5\sqrt{(1 \text{ GeV})/E_\nu}$ ) for the thick (thin) curves. In both panels, the right (left) curves correspond to the normal (inverted) ordering fit to a true inverted (normal) ordering.

Comparing red versus black curves with the same style shows the impact of the resolutions, whereas dashed versus solid curves with the same color shows the impact of systematics. From the comparison of thin versus thick curves we find that minimizing with respect to  $\theta_{13}$  and  $\theta_{23}$  has only a marginal impact on the sensitivity. Note, however, that in all cases we do minimize with respect to  $|\Delta m^2|$ , which is very important. By comparing the left and the right panel we find that a very similar behaviour is obtained by our two methods of taking into account reconstruction, either using only the muon or working with reconstructed neutrino parameters. In summary, for our setups, the ones with the best resolution and without systematic errors would have a sensitivity of around seven sigma after ten years of running; the sensitivity deteriorates to around three sigma if systematics are taken into account and only the more conservative assumptions on the resolutions can be satisfied.

It is well known that the sensitivity of atmospheric neutrino experiments to the neutrino mass ordering is quite dependent on the true value of the lepton mixing angle  $\theta_{23}$ . While there is so far no evidence for deviation of  $\theta_{23}$  from the maximal mixing value

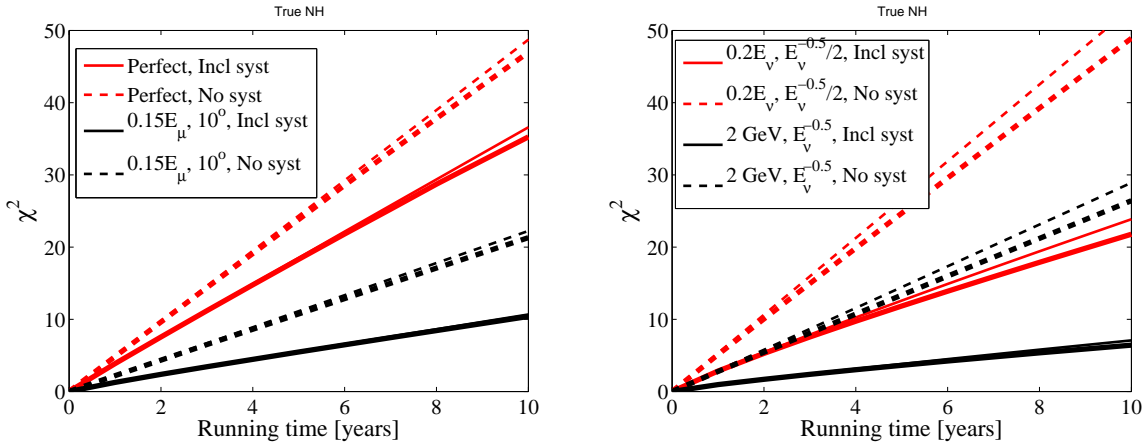


Figure 2: Time evolution of the PINGU mass ordering discovery potential for our different experimental assumptions on the energy and angular resolutions of the detector (see labeling in the figure). The left panel corresponds to using the muon parameters and the right panel to using the reconstructed neutrino parameters. The thin (thick) lines correspond to fixing (marginalizing) over  $\theta_{23}$  and  $\theta_{13}$ . All curves are marginalized with respect to  $|\Delta m_{31}^2|$  and we have assumed normal ordering to be true.

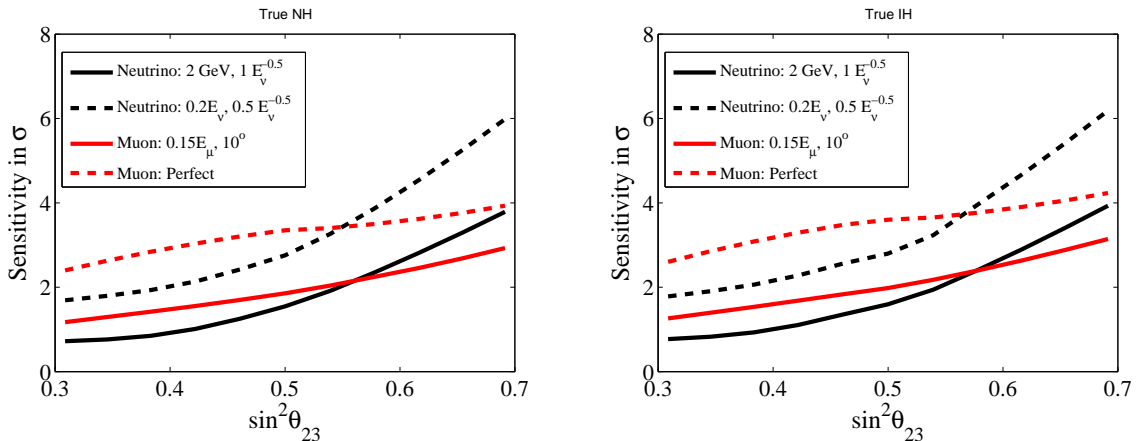


Figure 3: Dependence of the PINGU mass ordering sensitivity after 3 years on the true value of  $\theta_{23}$ . The sensitivity is defined as  $\sqrt{\Delta\chi^2}$ . The black (red) curves correspond to our setups studying the reconstructed neutrino (muon) parameters. The true neutrino mass ordering assumed to be normal (inverted) for the left (right) panel, and we include systematic effects as well as marginalization over the neutrino oscillation parameters. Dashed versus solid curves correspond to different assumptions on the resolutions as given in the legend.

$\pi/4$ , there are some hints at a level below two sigma that non-maximal values are preferred [11]. In Fig. 3, we show the dependence of the PINGU sensitivity on the true value of  $\sin^2 \theta_{23}$ . We find that, while the general trend of better sensitivity for  $\theta_{23}$  in the second octant observed in other studies is present, the size of the effect is strongly dependent not only on the assumptions we make on the detector resolutions, but also on whether we treat the problem using the muon or reconstructed neutrino parameters, with the reconstructed neutrino parameters gaining significantly in sensitivity for large values of  $\theta_{23}$ , while the muon parameter analysis shows a more modest gain. On a quantitative level, the sensitivity to the neutrino ordering as given by the reconstructed neutrino parameters changes by more than three sigma within the currently allowed range for  $\theta_{23}$ , from a low sensitivity of slightly below two sigma at  $\sin^2 \theta_{23} = 0.34$  to almost five sigma at  $\sin^2 \theta_{23} = 0.67$  (for the more optimistic assumption on the resolutions). For the analysis using the muon parameters, the difference in sensitivity between the extreme values of  $\theta_{23}$  is only around one and a half sigma. We interpret this behaviour such that the smearing affects  $\theta_{23}$  induced signatures in a slightly different way, depending on whether neutrino or muon quantities are used to describe the resolution. Since both approaches adopted here are approximate and should be replaced by realistic reconstruction algorithms based on Monte Carlo studies including detailed experimental information we do not investigate this behaviour further. We just conclude that also the  $\theta_{23}$  dependence of the sensitivity seems to depend crucially on the actual energy and direction reconstruction abilities of the detector. Let us mention also that by comparing the left and right panels we find that results are rather independent on whether the true ordering is normal or inverted.

Let us now relax the assumption  $\Delta m_{21}^2 = 0$  and consider the sensitivity when taking full three-flavour effects into account, including a non-zero  $\Delta m_{21}^2$  as well as the effect of the CP phase  $\delta$ . In Fig. 4 we show the  $\Delta\chi^2$  of the wrong mass ordering as a function of  $\delta$ , for various assumptions on the true CP phase. For this analysis only statistical errors are assumed and all other oscillation parameters except  $|\Delta m_{31}^2|$  are kept fixed. We observe that marginalizing over  $\delta$  has in impact of about 1 to 2 units in  $\Delta\chi^2$  for the exposure considered here (3 years). This corresponds roughly to a 10% effect on  $\Delta\chi^2$ . Note that this analysis is based on statistics only, hence, the  $\Delta\chi^2$  just scales linearly with exposure.

In passing let us comment on the possibility to constrain the CP phase with PINGU. The thin curves in Fig. 4 with the minimum at  $\Delta\chi^2 = 0$  correspond to the fit with the correct mass ordering. Those curves show that PINGU by itself will have very poor sensitivity to the CP phase. One may expect that systematic uncertainties will further reduce the sensitivity, even for  $\sim 10$  year exposures, see also [33].

### 3 Daya Bay II analysis

The possibility to use a precision measurement of the  $\bar{\nu}_e$  survival probability at a nuclear reactor to identify the neutrino mass ordering [23] has been considered by a number of

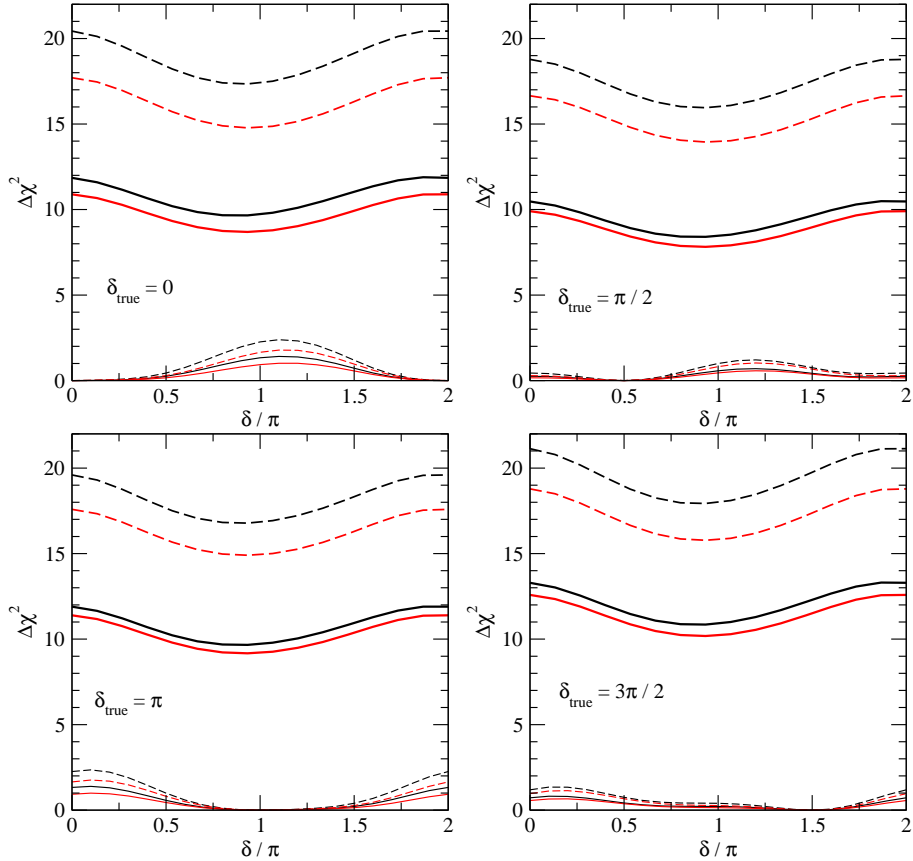


Figure 4:  $\Delta\chi^2$  as a function of the CP phase  $\delta$  for 3 years of PINGU data, for statistical errors only. We minimize with respect to  $|\Delta m_{31}^2|$ , all other oscillation parameters are fixed. The four panels correspond to true values of  $\delta = 0, \pi/2, \pi, 3\pi/2$ . Thin curves with the minimum at  $\Delta\chi^2 = 0$  correspond to the fit with the right mass ordering (normal), whereas the thick curves with non-zero minimum correspond to the wrong mass ordering (inverted). For black (red) curves the energy resolution is  $\sigma_{E_\nu} = 0.2\%$  (2 GeV), for solid (dashed) curves the angular resolution is  $\sigma_{\theta_\nu} = 1 (0.5) \times \sqrt{1 \text{ GeV}/E_\nu}$ .

authors [30–32, 58–68], boosted by the plans of the Daya Bay and RENO collaborations for such an experiment. For our sensitivity calculations for Daya Bay II we will follow [24, 25]. A 20 kt liquid scintillator detector is considered at a distance of 58 km from the reactors with a total power of 36 GW. The energy resolution is assumed to be  $3\% \sqrt{1 \text{ MeV}/E}$ . We normalize our number of events such that for an exposure of  $20 \text{ kt} \times 36 \text{ GW} \times 6 \text{ yr} = 4320 \text{ kt GW yr}$  we obtain  $10^5$  events [24, 25].

In our analysis we assume that the neutrino source is point-like at a distance of 58 km from the detector. We perform a  $\chi^2$  analysis using 350 bins for the energy spectrum. This number is chosen sufficiently large such that bins are smaller (or of the order of) the energy resolution. We take into account an overall normalization uncertainty of 5% and a linear energy scale uncertainty of 3%. Uncertainties in the oscillation parameters  $\sin^2 \theta_{13}$  and  $\sin^2 \theta_{12}$  are included as pull parameters in the  $\chi^2$  with  $\sigma(\sin^2 \theta_{13}) = 0.0023$

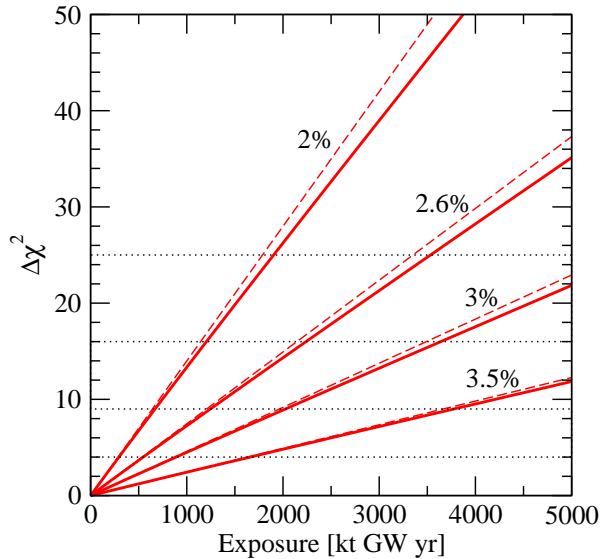


Figure 5:  $\Delta\chi^2$  of the wrong mass ordering for Daya Bay II as a function of the exposure for different assumptions on the energy resolution. The different set of curves correspond to energy resolutions of  $\sigma_E/E = a\sqrt{1\text{ MeV}/E}$ , with  $a = 2\%, 2.6\%, 3\%, 3.5\%$  as indicated in the plot. Dashed curves are for statistical errors only, solid curves include the uncertainty on normalization, linear energy scale,  $\sin^2\theta_{13}$ , and  $\sin^2\theta_{12}$ . We take  $\sin^2 2\theta_{13} = 0.089$  and minimize with respect to  $|\Delta m_{31}^2|$ .

and  $\sigma(\sin^2\theta_{12}) = 0.012$ . The  $\chi^2$  analysis and its interpretation is performed in complete analogy to the way described in section 2.2 for PINGU. With the above assumptions as well as  $\sin^2 2\theta_{13} = 0.089$  and 4320 kt GW yr we find a sensitivity to the mass ordering of  $\Delta\chi^2 = 19$ , which compares reasonably well to the value  $\Delta\chi^2 \approx 16$  found in [24,25,32]. Our results are also in reasonable agreement with [30,31] when we adopt the same assumptions as there, however, we obtain significantly weaker sensitivities as compared to [64,65].

In Fig. 5 we show the Daya Bay II sensitivity to the mass ordering as a function of the exposure, highlighting once more the well-known importance of the energy resolution. We observe that the systematical uncertainties considered here only play a sub-leading role. We note that these results are essentially independent of the assumed true ordering.

Let us point out that our analysis ignores some possible challenges of the experiment, such as the smearing induced by the contributions from reactor cores at slightly different baselines [32], the background from more distant nuclear power plants, or the effect of a non-linearity in the energy scale uncertainty [30]. While such issues have to be addressed in the actual analysis of such an experiment, our somewhat simplified treatment suffices to illustrate the power of the atmospheric/reactor combination.

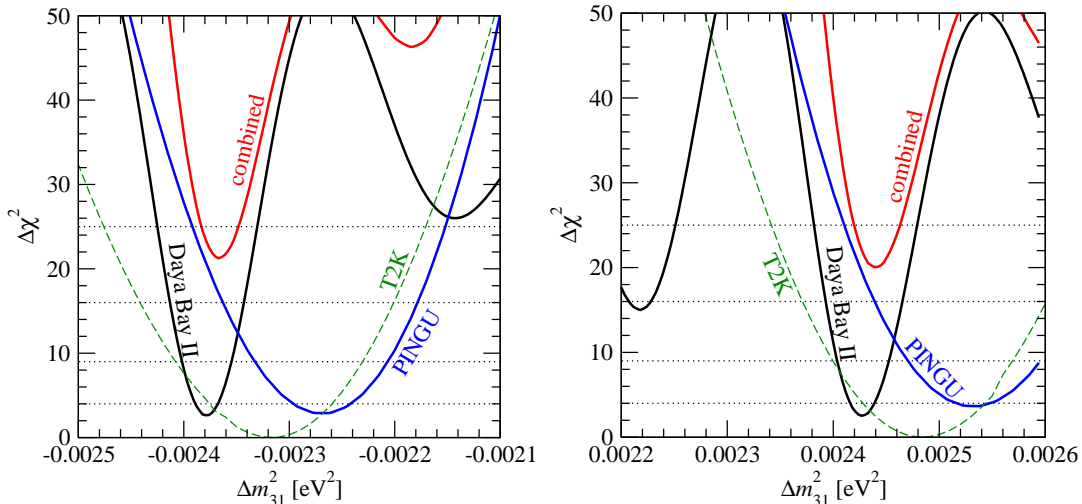


Figure 6:  $\Delta\chi^2$  as a function of  $\Delta m_{31}^2$  with the wrong sign for PINGU, Daya Bay II, and the combination. For PINGU we assume 1 year of data with  $\sigma_E = 2$  GeV and  $\sigma_{\theta_\nu} = \sqrt{1 \text{ GeV}/E_\nu}$ , statistical errors only, and we minimize with respect to  $\delta$  but keep all other oscillation parameters fixed. For Daya Bay II we take an exposure of 1000 kt GW yr and assume an energy resolution of  $\sigma_E = 3.5\% \sqrt{1 \text{ MeV}/E}$ . The dashed curves corresponds to 5 years of neutrino data at 0.77 MW from T2K (not included in the “combined” curve). We take the true values  $|\Delta m_{31}^2| = 2.4 \times 10^{-3} \text{ eV}^2$ ,  $\sin^2 2\theta_{13} = 0.092$ ,  $\sin^2 \theta_{23} = 0.5$ ,  $\delta = 0$ ,  $\Delta m_{21}^2 = 7.59 \cdot 10^{-5} \text{ eV}^2$ . For the left (right) panel the true mass ordering is normal (inverted).

## 4 Combination of PINGU and Daya Bay II

We now move to the main point of this work, the combination of data from a high-statistics atmospheric and a medium-baseline reactor experiment. For our combined analysis of PINGU and Daya Bay II, we need to consider the full three flavor framework in order to properly assess the combined sensitivity. This is due to the fact that the effect we are exploiting is mainly based on the impact of  $\Delta m_{21}^2$  on the best fit of  $\Delta m_{31}^2$  for the wrong ordering. It is therefore necessary to take three flavour oscillations into account without approximation in order to obtain reliable results. For computational reasons we neglect the impact of systematic uncertainties in PINGU, however we will comment on their impact later in this section.

The basic mechanism is illustrated in Fig. 6. We show the power of combining PINGU and Daya Bay II results by plotting the individual  $\Delta\chi^2$  as well as their sum as a function of the wrong sign  $\Delta m_{31}^2$ . With the parameters chosen for this plot neither of the experiments would have a sensitivity to the neutrino mass ordering of more than two sigma. However, the  $|\Delta m_{31}^2|$  best fit values would differ significantly. This implies that the overall best fit occurs at a value of  $|\Delta m_{31}^2|$  which is not advantageous for either of the experiments and therefore the sensitivity increases significantly, as can be seen from the red curve, to between four and five sigma.

We can estimate the synergy effect in the following way: Let us denote the individual  $\Delta\chi^2$  functions as  $\Delta\chi_i^2(x)$ , with  $i = 1, 2$ , corresponding to PINGU and Daya Bay II, respectively, and  $x$  denoting  $|\Delta m_{31}^2|$  in the wrong mass ordering. Close to the minimum we can approximate the  $\Delta\chi^2$  by a parabola and we write

$$\Delta\chi_i^2(x) = \chi_{i,\min}^2 + \left( \frac{x - x_{0,i}}{\sigma_i} \right)^2, \quad (6)$$

where  $x_{0,i}$  denotes the best fit value for  $|\Delta m_{31}^2|$  in the wrong mass ordering and  $\sigma_i$  the corresponding  $1\sigma$  error for experiment  $i$ . The minimum of the combined  $\chi^2$  is then obtained as

$$\Delta\chi_{\text{comb}}^2 = \chi_{1,\min}^2 + \chi_{2,\min}^2 + \frac{(x_{0,1} - x_{0,2})^2}{\sigma_1^2 + \sigma_2^2}. \quad (7)$$

The first two terms correspond to the individual mass ordering sensitivities of the two experiments, whereas the last term takes into account the synergy effect from the mismatch of the different  $\Delta m_{31}^2$  best fit values. We observe that, if the best fit points differ by more than the respective uncertainties summed in square, a relevant synergy is obtained from the combination. Eq. 7 assumes that the parabolic shape of the individual  $\chi^2$  functions is still valid at the location of the combined best fit point, which may not be true if it is located far away (in units of  $\sigma_i$ ) from one of the individual minima. In such a situation eq. 7 does not apply and the actual  $\chi^2$  profiles have to be used. Note also that eq. 7 ignores additional correlations due to the dependence on other oscillation parameters (apart from  $|\Delta m_{31}^2|$ ), which are, however, expected to be small.

In Fig. 7 we show how the best fit points for  $|\Delta m_{31}^2|$  and its accuracy depend on experimental parameters for Daya Bay II and PINGU. We observe that the location of the minima are relatively stable with respect to resolutions, and the difference between the best fit points with the wrong sign of  $\Delta m_{31}^2$  remains at the level of  $\gtrsim 0.1 \cdot 10^{-3} \text{ eV}^2$ . However, the accuracy on  $|\Delta m_{31}^2|$  (especially from PINGU) is affected by resolutions. For the chosen parameters an angular reconstruction in PINGU better than about  $2\sqrt{1 \text{ GeV}/E_\nu}$  is required to obtain a sufficient accuracy on  $\Delta m_{31}^2$ . In the upper panels we show the individual sensitivities to the mass ordering. It is clear that the synergy effect can be used to exclude the wrong mass ordering in a regime where the individual experiments achieve only a poor rejection power. This is particularly true for Daya Bay II: while the  $\Delta\chi^2$  from Daya Bay II alone is severely affected by the energy resolution, the accuracy on  $|\Delta m_{31}^2|$  in the wrong ordering remains excellent, see also [59]. For instance even for an energy resolution of 6%, where the sensitivity to the mass ordering completely disappears, an accuracy of  $\sigma(|\Delta m_{31}^2|) \approx 0.02 \cdot 10^{-3} \text{ eV}^2$  is achieved, still much smaller than the typical difference between the PINGU and Daya Bay II best fit points, which are of order  $0.1 \cdot 10^{-3} \text{ eV}^2$ .

We note that for this plot only modest exposure times are assumed, corresponding to 1 year of PINGU data and about 1.3 years reactor data for a 20 kt detector at a 36 GW power plant. For the analysis used in Fig. 7 the accuracy on  $|\Delta m_{31}^2|$  would scale with the square-root of the exposure for Daya Bay II as well as for PINGU.

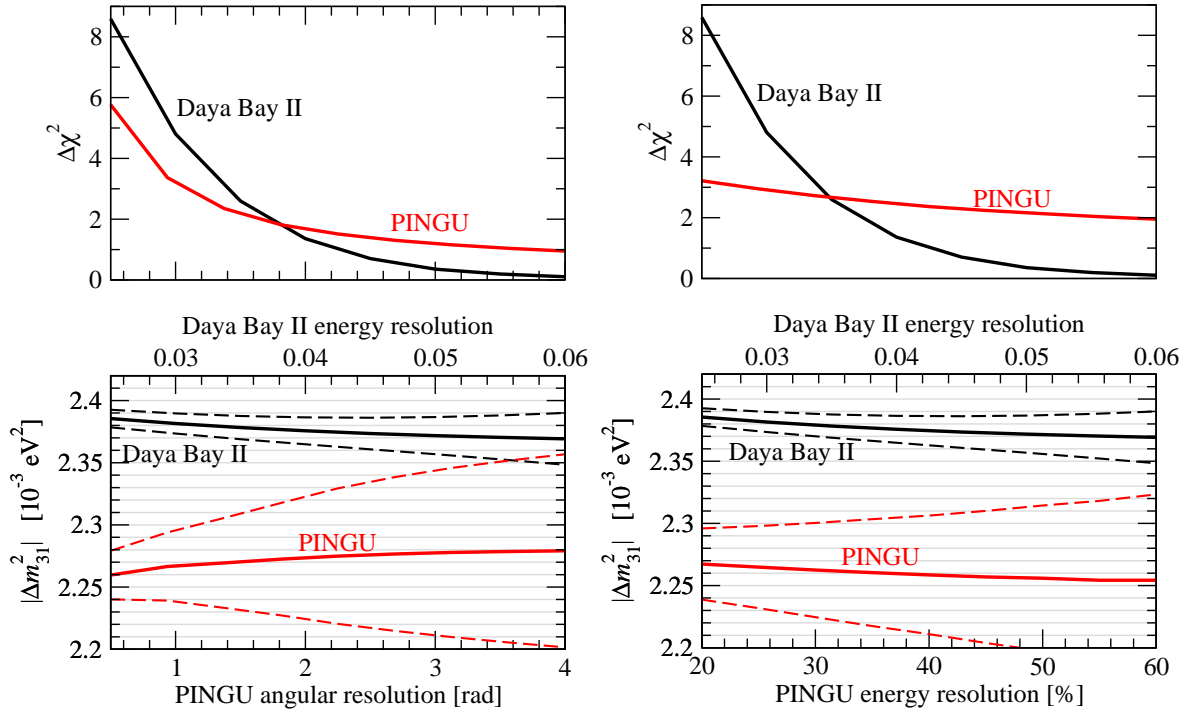


Figure 7: Lower panels: the best fit (solid) and  $1\sigma$  range (dashed) for  $|\Delta m_{31}^2|$  for the wrong mass ordering. For Daya Bay II we show it as a function of the energy resolution parameter  $a$ , where  $\sigma_E/E_\nu = a\sqrt{1 \text{ MeV}/E}$  (upper horizontal axis). The exposure is 1000 kt GW yr. For PINGU we use the parametrization from eq. 2. In the left panel we take  $A = 0$ ,  $B = 0.2$ ,  $C$  is shown on the lower horizontal axis; in the right panel we take  $A = 0$ ,  $B$  is shown on the lower horizontal axis,  $C = 1$ . The PINGU exposure is 1 year. In the upper panels we show the correspond  $\Delta\chi^2$  for PINGU and Daya Bay II alone. The true values are  $\Delta m_{31}^2 = 2.4 \cdot 10^{-3} \text{ eV}^2$  (normal ordering),  $\sin^2 2\theta_{13} = 0.092$  and other parameters as in eq. 5. For PINGU we consider statistical errors only and we marginalize with respect to  $\delta$ , all other oscillation parameters are fixed.

We have checked that the accuracy on  $|\Delta m_{31}^2|$  as well as its best fit value for the wrong ordering from PINGU depends very little on the true value of  $\theta_{23}$ . Hence, the combined analysis with Daya Bay II remains unaffected by the value of  $\theta_{23}$ , whereas the PINGU sensitivity to the mass ordering depends crucially on  $\theta_{23}$ , as we have seen in Fig. 3.

In Fig. 6 we show as dashed curves also the accuracy obtainable by the T2K long-baseline experiment [69]. We use GLoBES [70, 71] to simulate T2K and assume 5 years of neutrino data at a beam power of 0.77 MW and we consider only the  $\nu_\mu$  disappearance channel, since we are interested here in the obtainable accuracy on  $|\Delta m_{31}^2|$ . We find a minor synergy of Daya Bay II also with T2K, although the effect is much less significant compared to PINGU. We also observe that the minimum of the wrong ordering appears for T2K at a slightly different location than for PINGU, indicating that the matter effect plays an important role in determining the best fit value of  $|\Delta m_{31}^2|$  with the wrong sign.

Let us comment also on a possible synergy of Daya Bay II with the INO atmospheric neutrino experiment [16]. Using our results from [17] we obtain an accuracy on  $|\Delta m_{31}^2|$  of  $0.076 (0.054) \cdot 10^{-3} \text{ eV}^2$  for a 10 year exposure of a 50 kt (100 kt) detector, assuming the “optimistic” resolutions from [17]. While those accuracies are worse than the ones we find for PINGU (depending on the resolutions) they are still comparable to the difference in the  $|\Delta m_{31}^2|$  best fit points and at some level a synergy effect may also emerge from the combination of Daya Bay II and INO. In [18] a slightly worse accuracy of about  $0.12 \cdot 10^{-3} \text{ eV}^2$  has been obtained for a 10 year exposure of a 50 kt detector. A detailed numerical study of the INO/Daya Bay II combination is beyond the scope of this work.

Let us now comment on the possible impact of systematic uncertainties on the PINGU result. This can be deduced from Fig. 1. This figure has been obtained in the approximation  $\Delta m_{21}^2 = 0$  and therefore those results cannot be directly used for the PINGU/Daya Bay II comparison. However, we note that the best fit in the wrong ordering occurs for values of  $|\Delta m^2|$  smaller (larger) than the simulated  $2.4 \cdot 10^{-3} \text{ eV}^2$  for a true normal (inverted) ordering, although we used the approximation  $\Delta m_{21}^2 = 0$ . This shows that the physics involved here are fundamentally different from the effect discussed in [27, 28] and rather depends on how the matter effect comes into play. The final result will of course depend on the matter effect as well as on  $\Delta m_{21}^2$  effects. Indeed, both effects move the best fit in the same direction and will therefore synergize to provide an even better sensitivity when considering PINGU and Daya Bay II together. This can be appreciated by comparing the locations of the  $\chi^2$  minima in Figs. 1 and 6, the latter showing much larger deviations from the value assumed in the true mass ordering ( $2.4 \cdot 10^{-3} \text{ eV}^2$ ).

Nevertheless, we can use the results from Fig. 1 to estimate the impact of systematical errors. We find that the inclusion of systematical errors into the PINGU analysis does neither change the location of the minimum in  $|\Delta m_{31}^2|$  nor the accuracy of its determination. Instead, the main effect is a shift of the  $\Delta\chi^2$ , modifying the mass ordering sensitivity of PINGU alone. We have numerically verified that using reconstructed neutrino parameters the value of  $|\Delta m^2|$  at the minimum remains unaffected up to the sub-percent level, and the accuracy remains constant at a values of  $\sigma(|\Delta m^2|) = 0.011 (0.014) \cdot 10^{-3} \text{ eV}^2$  for resolutions according to eq. 2 of  $A = 0 (2 \text{ GeV})$ ,  $B = 0.2 (0)$ ,  $C = 0.5 (1)$ . For using muon reconstruction parameters the error is between  $0.018$  and  $0.020 \cdot 10^{-3} \text{ eV}^2$  for the finite resolutions and between  $0.013$  and  $0.014 \cdot 10^{-3} \text{ eV}^2$  for perfect muon resolutions (these numbers correspond to a 3 year exposure, as adopted in Fig. 1). Thus, the inclusion of systematics into the PINGU analysis would not significantly affect the outcome apart from shifting the PINGU and combined curves of Fig. 6 down by an amount of at most the PINGU sensitivity while the synergy effect of the PINGU/Daya Bay II combination remains unaffected.

## 5 Conclusions

In this work we pointed out a synergy for the determination of the neutrino mass ordering between atmospheric neutrino data in low-energy extensions of neutrino telescopes such as PINGU or ORCA and a medium-baseline reactor neutrino experiment such as Daya Bay II or RENO50. Identifying the mass ordering is a rather challenging task for those type of experiments and we may face the unfortunate situation that each of them reaches only a poor sensitivity. One reason for the difficulty is that it is possible to obtain a reasonable fit within the wrong mass ordering by adjusting the value of  $|\Delta m_{31}^2|$ . However, the oscillation physics in the atmospheric and reactor neutrino experiments are very different. In the first case a complicated superposition of oscillation channels is observed and a major role is played by the matter effect in the earth, while in the second case tiny wiggles in the energy spectrum due to the  $\bar{\nu}_e$  survival probability in vacuum are used. Hence, the values of  $|\Delta m_{31}^2|$  which may fake the wrong mass ordering are expected to be different in the two type of experiments. Our numerical analysis shows that the best fit values of  $|\Delta m_{31}^2|$  typically differ by about  $0.1 \cdot 10^{-3} \text{ eV}^2$ . This is large compared to the rather impressive accuracy with which  $|\Delta m_{31}^2|$  will be determined by those experiments, which is typically in the range between 0.01 and  $0.02 \cdot 10^{-3} \text{ eV}^2$ . Hence, it may be possible to exclude the wrong mass ordering due to the mismatch of the best fit values for  $\Delta m_{31}^2$  in the two type of experiments, even if each experiment on its own cannot.

We have performed some preliminary estimates on how the value and the accuracy of  $|\Delta m_{31}^2|$  in the wrong ordering are affected by experimental parameters such as energy resolutions, directional reconstruction of atmospheric neutrinos, systematical uncertainties, and exposure. Our results indicate that for experimental parameters similar to the ones discussed for the PINGU and ORCA proposals, as well as those for Daya Bay II and RENO50, the synergy effect in a combined analysis will boost the mass ordering sensitivity significantly. The experimental requirements are somewhat relaxed compared to those of the individual sensitivities. Our results will need to be confirmed by more realistic simulations once detailed reconstruction abilities and experimental uncertainties of the respective experiments become available.

While the sensitivity of atmospheric neutrinos to the mass ordering strongly depends on the true value of  $\theta_{23}$  (better sensitivity for larger  $\theta_{23}$ ) the synergy effect with the reactor data does not depend on  $\theta_{23}$ . In this respect, the sensitivity of the combined reactor and atmospheric neutrino analysis is stable against the uncertainty introduced by the unknown true value of  $\theta_{23}$ .

In conclusion, the combined analysis of atmospheric and reactor neutrino experiments proposed here may be the only way to identify the mass ordering if the individual experiments can only achieve poor sensitivities, or the mass ordering may be identified already after a much shorter running time of the experiments. Certainly the comparison of the  $|\Delta m_{31}^2|$  measurement in different experiments will provide an important cross check for any mass ordering determination. Perhaps the combined sensitivity of (*i*) the earth mat-

ter effect, (ii) subtle interference terms in the vacuum  $\bar{\nu}_e$  survival probability, and (iii) the comparison of  $|\Delta m_{31}^2|$  measurements in different experiments may finally determine the sign of  $\Delta m_{31}^2$  beyond doubt.

**Acknowledgment.** We thank Davide Franco and Anselmo Mereaglia for intense exchanges in an early stage of this work and Alexei Smirnov for discussions. We are grateful to Ken Clark for providing information on PINGU. We thank Sandhya Choubey for pointing out an important typo in an earlier version of this manuscript. This work was supported by the Göran Gustafsson Foundation (M.B.). T.S. acknowledges partial support from the European Union FP7 ITN INVISIBLES (Marie Curie Actions, PITN-GA-2011-289442).

**Note added.** After the completion of this work the Daya Bay II project has been named JUNO (Jiangmen Underground Neutrino Observatory), see e.g., [72].

## References

- [1] Super-Kamiokande, Y. Fukuda *et al.*, *Evidence for oscillation of atmospheric neutrinos*, Phys. Rev. Lett. **81**, 1562 (1998), hep-ex/9807003.
- [2] KamLAND Collaboration, K. Eguchi *et al.*, *First results from KamLAND: Evidence for reactor anti-neutrino disappearance*, Phys.Rev.Lett. **90**, 021802 (2003), hep-ex/0212021.
- [3] KamLAND, T. Araki *et al.*, *Measurement of neutrino oscillation with KamLAND: Evidence of spectral distortion*, Phys. Rev. Lett. **94**, 081801 (2005), hep-ex/0406035.
- [4] CHOOZ Collaboration, M. Apollonio *et al.*, *Search for neutrino oscillations on a long baseline at the CHOOZ nuclear power station*, Eur.Phys.J. **C27**, 331 (2003), hep-ex/0301017.
- [5] DAYA-BAY, F. An *et al.*, *Observation of electron-antineutrino disappearance at Daya Bay*, Phys.Rev.Lett. **108**, 171803 (2012), 1203.1669.
- [6] RENO, J. Ahn *et al.*, *Observation of Reactor Electron Antineutrino Disappearance in the RENO Experiment*, Phys.Rev.Lett. **108**, 191802 (2012), 1204.0626.
- [7] Double Chooz, Y. Abe *et al.*, *Reactor electron antineutrino disappearance in the Double Chooz experiment*, Phys.Rev. **D86**, 052008 (2012), 1207.6632.
- [8] SNO, Q. R. Ahmad *et al.*, *Direct evidence for neutrino flavor transformation from neutral-current interactions in the Sudbury Neutrino Observatory*, Phys. Rev. Lett. **89**, 011301 (2002), nucl-ex/0204008.
- [9] MINOS, P. Adamson *et al.*, *Measurement of Neutrino Oscillations with the MINOS Detectors in the NuMI Beam*, Phys. Rev. Lett. **101**, 131802 (2008), 0806.2237.

- [10] T2K, K. Abe *et al.*, *Indication of Electron Neutrino Appearance from an Accelerator-produced Off-axis Muon Neutrino Beam*, Phys.Rev.Lett. **107**, 041801 (2011), 1106.2822.
- [11] M. Gonzalez-Garcia, M. Maltoni, J. Salvado, and T. Schwetz, *Global fit to three neutrino mixing: critical look at present precision*, JHEP **1212**, 123 (2012), 1209.3023, updated results available at <http://www.nu-fit.org>.
- [12] L. Wolfenstein, *Neutrino Oscillations in Matter*, Phys.Rev. **D17**, 2369 (1978).
- [13] V. D. Barger, K. Whisnant, S. Pakvasa, and R. Phillips, *Matter Effects on Three-Neutrino Oscillations*, Phys.Rev. **D22**, 2718 (1980).
- [14] S. Mikheev and A. Smirnov, *Resonance Amplification of Oscillations in Matter and Spectroscopy of Solar Neutrinos*, Sov.J.Nucl.Phys. **42**, 913 (1985).
- [15] M. Blennow and A. Y. Smirnov, *Neutrino propagation in matter*, Adv.High Energy Phys. **2013**, 972485 (2013), 1306.2903.
- [16] INO, India-Based Neutrino Observatory, <http://www.ino.tifr.res.in/ino/>
- [17] M. Blennow and T. Schwetz, *Identifying the Neutrino mass Ordering with INO and NOvA*, JHEP **1208**, 058 (2012), 1203.3388.
- [18] A. Ghosh, T. Thakore, and S. Choubey, *Determining the Neutrino Mass Hierarchy with INO, T2K, NOvA and Reactor Experiments*, JHEP **1304**, 009 (2013), 1212.1305.
- [19] D. J. Koskinen, *IceCube-DeepCore-PINGU: Fundamental neutrino and dark matter physics at the South Pole*, Mod.Phys.Lett. **A26**, 2899 (2011).
- [20] Km3Net, P. Coyle *et al.*, , (2012), contribution to the European Strategy Preparatory Group Symposium, September 2012 Krakow, Poland.
- [21] K. Abe *et al.*, *Letter of Intent: The Hyper-Kamiokande Experiment — Detector Design and Physics Potential*, (2011), 1109.3262.
- [22] D. Autiero *et al.*, *Large underground, liquid based detectors for astro-particle physics in Europe: Scientific case and prospects*, JCAP **0711**, 011 (2007), 0705.0116.
- [23] S. Petcov and M. Piai, *The LMA MSW solution of the solar neutrino problem, inverted neutrino mass hierarchy and reactor neutrino experiments*, Phys.Lett. **B533**, 94 (2002), hep-ph/0112074.
- [24] Y. Wang, *Daya Bay II: current status and future plan*, talk at Daya Bay II meeting, IHEP Jan 11, 2013.
- [25] W. Wang, *The Measurement of  $\theta_{13}$  at Daya Bay and Beyond*, talk at the "Beyond  $\theta_{13}$ " workshop, Univ. Pittsburgh, 11-12 Feb. 2013, <http://www.pitt.edu/~neilc/BeyondTheta13/>
- [26] International Workshop on "RENO-50" toward Neutrino Mass Hierarchy, 13-14 June 2013, Seoul National University, Korea, <http://home.kias.re.kr/MKG/h/reno50/>

- [27] H. Nunokawa, S. J. Parke, and R. Zukanovich Funchal, *Another possible way to determine the neutrino mass hierarchy*, Phys. Rev. **D72**, 013009 (2005), hep-ph/0503283.
- [28] H. Minakata, H. Nunokawa, S. J. Parke, and R. Zukanovich Funchal, *Determining neutrino mass hierarchy by precision measurements in electron and muon neutrino disappearance experiments*, Phys.Rev. **D74**, 053008 (2006), hep-ph/0607284.
- [29] A. de Gouvea, J. Jenkins, and B. Kayser, *Neutrino mass hierarchy, vacuum oscillations, and vanishing  $|U_{e3}|$* , Phys.Rev. **D71**, 113009 (2005), hep-ph/0503079.
- [30] X. Qian *et al.*, *Mass Hierarchy Resolution in Reactor Anti-neutrino Experiments: Parameter Degeneracies and Detector Energy Response*, PRD, 87, **033005** (2013), 1208.1551.
- [31] S.-F. Ge, K. Hagiwara, N. Okamura, and Y. Takaesu, *Determination of mass hierarchy with medium baseline reactor neutrino experiments*, JHEP **1305**, 131 (2013), 1210.8141.
- [32] Y.-F. Li, J. Cao, Y. Wang, and L. Zhan, *Unambiguous Determination of the Neutrino Mass Hierarchy Using Reactor Neutrinos*, (2013), 1303.6733.
- [33] W. Winter, *Neutrino mass hierarchy determination with IceCube-PINGU*, (2013), 1305.5539.
- [34] IceCube Collaboration, R. Abbasi *et al.*, *The Design and Performance of IceCube DeepCore*, Astropart.Phys. **35**, 615 (2012), 1109.6096.
- [35] D. Fargion, D. D'Armiento, P. Desiati, and P. Paggi, *Beaming neutrino and antineutrinos across the Earth to disentangle neutrino mixing parameters*, Astrophys.J. **758**, 3 (2012), 1012.3245.
- [36] J. Tang and W. Winter, *Requirements for a New Detector at the South Pole Receiving an Accelerator Neutrino Beam*, JHEP **1202**, 028 (2012), 1110.5908.
- [37] J. Brunner, *Counting Electrons to Probe the Neutrino Mass Hierarchy*, (2013), 1304.6230.
- [38] E. K. Akhmedov, S. Razzaque, and A. Y. Smirnov, *Mass hierarchy, 2-3 mixing and CP-phase with Huge Atmospheric Neutrino Detectors*, JHEP **02**, 082 (2013), 1205.7071.
- [39] O. Mena, I. Mocioiu, and S. Razzaque, *Neutrino mass hierarchy extraction using atmospheric neutrinos in ice*, Phys. Rev. **D78**, 093003 (2008), 0803.3044.
- [40] E. Fernandez-Martinez, G. Giordano, O. Mena, and I. Mocioiu, *Atmospheric neutrinos in ice and measurement of neutrino oscillation parameters*, Phys.Rev. **D82**, 093011 (2010), 1008.4783.
- [41] D. Indumathi and M. Murthy, *A Question of hierarchy: Matter effects with atmospheric neutrinos and anti-neutrinos*, Phys.Rev. **D71**, 013001 (2005), hep-ph/0407336.

- [42] S. Petcov and T. Schwetz, *Determining the neutrino mass hierarchy with atmospheric neutrinos*, Nucl.Phys. **B740**, 1 (2006), hep-ph/0511277.
- [43] A. Samanta, *The Mass hierarchy with atmospheric neutrinos at INO*, Phys.Lett. **B673**, 37 (2009), hep-ph/0610196.
- [44] S. K. Agarwalla, T. Li, O. Mena, and S. Palomares-Ruiz, *Exploring the Earth matter effect with atmospheric neutrinos in ice*, (2012), 1212.2238.
- [45] D. Franco *et al.*, *Mass hierarchy discrimination with atmospheric neutrinos in large volume ice/water Cherenkov detectors*, JHEP **1304**, 008 (2013), 1301.4332.
- [46] M. Ribordy and A. Y. Smirnov, *Improving the neutrino mass hierarchy identification with inelasticity measurement in PINGU and ORCA*, (2013), 1303.0758.
- [47] D. Cowen, *Future Instruments: PINGU*, (2013), talk at Snowmass Cosmic Frontier Workshop, 6–8 March, 2013, SLAC, USA.
- [48] A. Dziewonski and D. Anderson, *Preliminary reference earth model*, Phys.Earth Planet.Interiors **25**, 297 (1981).
- [49] M. Honda, T. Kajita, K. Kasahara, and S. Midorikawa, *Calculation of the flux of atmospheric neutrinos*, Phys.Rev. **D52**, 4985 (1995), hep-ph/9503439.
- [50] C. Andreopoulos *et al.*, *The GENIE Neutrino Monte Carlo Generator*, Nucl.Instrum.Meth. **A614**, 87 (2010), 0905.2517.
- [51] A. Ghosh and S. Choubey, *Measuring the Mass Hierarchy with Muon and Hadron Events in Atmospheric Neutrino Experiments*, (2013), 1306.1423.
- [52] M. Honda, T. Kajita, K. Kasahara, and S. Midorikawa, *A New calculation of the atmospheric neutrino flux in a 3-dimensional scheme*, Phys.Rev. **D70**, 043008 (2004), astro-ph/0404457.
- [53] E. A. Paschos and J. Y. Yu, *Neutrino interactions in oscillation experiments*, Phys. Rev. **D65**, 033002 (2002), hep-ph/0107261.
- [54] M. Gonzalez-Garcia and M. Maltoni, *Atmospheric neutrino oscillations and new physics*, Phys.Rev. **D70**, 033010 (2004), hep-ph/0404085.
- [55] M. Blennow, P. Coloma, P. Huber, and T. Schwetz, (2013), in preparation.
- [56] X. Qian *et al.*, *Statistical Evaluation of Experimental Determinations of Neutrino Mass Hierarchy*, Phys.Rev. **D86**, 113011 (2012), 1210.3651.
- [57] E. Ciuffoli, J. Evslin, and X. Zhang, *Confidence in a Neutrino Mass Hierarchy Determination*, (2013), 1305.5150.
- [58] S. Schonert, T. Lasserre, and L. Oberauer, *The HLMA project: Determination of high  $\Delta m^2$  LMA mixing parameters and constraint on  $|U_{e3}|$  with a new reactor neutrino experiment*, Astropart.Phys. **18**, 565 (2003), hep-ex/0203013.

- [59] S. Choubey, S. Petcov, and M. Piai, *Precision neutrino oscillation physics with an intermediate baseline reactor neutrino experiment*, Phys.Rev. **D68**, 113006 (2003), hep-ph/0306017.
- [60] J. Learned, S. T. Dye, S. Pakvasa, and R. C. Svoboda, *Determination of neutrino mass hierarchy and  $\theta(13)$  with a remote detector of reactor antineutrinos*, Phys.Rev. **D78**, 071302 (2008), hep-ex/0612022.
- [61] M. Batygov *et al.*, *Prospects of neutrino oscillation measurements in the detection of reactor antineutrinos with a medium-baseline experiment*, (2008), 0810.2580.
- [62] L. Zhan, Y. Wang, J. Cao, and L. Wen, *Determination of the Neutrino Mass Hierarchy at an Intermediate Baseline*, Phys.Rev. **D78**, 111103 (2008), 0807.3203.
- [63] L. Zhan, Y. Wang, J. Cao, and L. Wen, *Experimental Requirements to Determine the Neutrino Mass Hierarchy Using Reactor Neutrinos*, Phys.Rev. **D79**, 073007 (2009), 0901.2976.
- [64] P. Ghoshal and S. Petcov, *Neutrino Mass Hierarchy Determination Using Reactor Antineutrinos*, JHEP **1103**, 058 (2011), 1011.1646.
- [65] P. Ghoshal and S. Petcov, *Addendum: Neutrino Mass Hierarchy Determination Using Reactor Antineutrinos*, JHEP **1209**, 115 (2012), 1208.6473.
- [66] E. Ciuffoli, J. Evslin, and X. Zhang, *Mass Hierarchy Determination Using Neutrinos from Multiple Reactors*, JHEP **1212**, 004 (2012), 1209.2227.
- [67] E. Ciuffoli *et al.*, *Medium Baseline Reactor Neutrino Experiments with 2 Identical Detectors*, (2012), 1211.6818.
- [68] E. Ciuffoli, J. Evslin, and X. Zhang, *Optimizing Medium Baseline Reactor Neutrino Experiments*, (2013), 1302.0624.
- [69] T2K Collaboration, K. Abe *et al.*, *First Muon-Neutrino Disappearance Study with an Off-Axis Beam*, Phys.Rev. **D85**, 031103 (2012), 1201.1386.
- [70] P. Huber, M. Lindner, and W. Winter, *Simulation of long-baseline neutrino oscillation experiments with GLoBES (General Long Baseline Experiment Simulator)*, Comput.Phys.Commun. **167**, 195 (2005), hep-ph/0407333.
- [71] P. Huber, J. Kopp, M. Lindner, M. Rolinec, and W. Winter, *New features in the simulation of neutrino oscillation experiments with GLoBES 3.0: General Long Baseline Experiment Simulator*, Comput.Phys.Commun. **177**, 432 (2007), hep-ph/0701187.
- [72] W. Wang, *Resolving Neutrino Mass Hierarchy using Nuclear Reactor(s)*, talk at Invisibles'13, Lumley Castle, July 16, 2013.